Ultrafast Dynamics of Room Temperature Ionic Liquids after Ultraviolet Femtosecond Excitation†

H. Brands, N. Chandrasekhar, and A.-N. Unterreiner*

Institut für Physikalische Chemie, Lehrstuhl für Molekulare Physikalische Chemie, Universität Karlsruhe, Kaiserstr. 12, D-76128 Karlsruhe, Germany

Received: October 31, 2006; In Final Form: December 19, 2006

The photochemistry and relaxation dynamics of four room-temperature ionic liquids (RTILs) after ultraviolet (UV) photolysis were investigated by femtosecond pump−probe absorption spectroscopy. A pulse duration-limited rise of the induced absorption in halide-containing RTILs at various probe wavelengths was attributed to the generation of solvated electrons. With continuous irradiation (static conditions), di- and trihalide ion formation became apparent especially below 1000 nm. The formation of trihalide ions was further confirmed by steady-state UV absorption spectroscopy. All RTILs showed a rich photochemistry after UV photolysis leading to the build-up of various long-lived intermediate products as evidenced from the observation that ionic liquids turn yellow upon continuous irradiation. On the other hand, exposing RTILs to the excitation pulse for a short time (rapid-scan method) significantly suppressed the formation of halides. The results suggest that the development of flow-cell systems for highly viscous ionic liquids is urgently needed to quantitatively investigate their ultrafast dynamics.

1. Introduction

It is known that solvated electrons in room-temperature ionic liquids (RTILs) can be generated either by pulse radiolysis[1−3] or by direct photoionization[4,5] of RTILs. While the peak position of their absorption spectra depends strongly on the nature of the cation and the substituent groups, the solvation dynamics are much slower in IL alcohols compared to ordinary alcohols.[1] In our previous studies,[4,5] solvated electrons were generated by direct photolysis of neat and doped ILs based on phosphonium and pyrrolidinium cations with a femtosecond laser pulse at 266 nm. The rise of the induced absorption after photoexcitation (time resolution $\approx$ 150 fs) was attributed to the formation of solvated electrons. It was further shown that when ILs were doped with various salts such as dimethylpyrrolidinium iodide or tetra-*n*-butylammonium iodide (TBAI) an increase of the yield of solvated electrons was observed and the relaxation dynamics were found to be independent of the nature of the dopant and probe wavelengths.[4] From these results it was concluded that solvated electrons can be generated both by direct one-photon ionization of the anion in RTILs (in this case the amide) and by photodetachment of iodide. It was also shown[4] that in pure ILs solvated electrons localize upon excitation within the time resolution of the experimental setup indicating the existence of preformed holes in which the electron localizes. In contrast, a delayed formation of solvated electrons in doped RTILs (0.5 mol/L salt concentration) was found where the induced absorption peaked around 2 ps after the excitation pulse. The delayed formation of solvated electrons in doped RTILs may be an indication of an occupation of holes by the doped iodide ions. While the induced absorption in pure RTILs remained more or less unchanged over hundreds of picoseconds after an initial small decay (~20%) with a time constant of about 1 ps, more than 80% decayed within 2 ps in doped RTILs, suggesting an efficient geminate recombination.[4]

Since RTILs—especially those based on imidazolium cations—have recently been considered as future solvents in many chemical and industrial applications,[6−13] particularly in solar cells,[14−19] it is pertinent to carry out investigations on the earliest steps of the photochemistry of RTILs in order to better understand reaction pathways in these liquids. While the efficiency of dye-sensitized solar cells in converting solar into chemical energy was reported to be lower compared to conventional organic solvents, their stability and performance were found to be better.[20,21] Therefore, studies of the relaxation dynamics of RTILs require further efforts for a more detailed picture.[22] As we will show here, it may be also worthwhile investigating RTILs in terms of their chemical stability under intense UV irradiation. Furthermore, using solvated electrons as a probe allows an investigation of the relaxation dynamics in pure and doped ILs with the help of femtosecond laser spectroscopy. In the present study various pure and doped RTILs such as 1-butyl-1-methylpyrrolidinium bis(trifluoromethylsulfonyl)amide, [bmPyr][NTf_2], trihexyltetradecylphosphonium bis(trifluoromethylsulfonyl)amide, [R_4P][NTf_2], 1-butyl-3-methylimidazolium iodide, [bmim]I, and 1-hexyl-3-methyl-imidazolium chloride, [hmim]Cl, have been used to investigate the photoinduced relaxation dynamics of solvated electrons with the help of femtosecond pump−probe spectroscopy. The latter two ILs were chosen with different anions to quantitatively test the recombination efficiency of solvated electrons as a function of halide atoms.

2. Experimental

A complete description of our two laser systems employed in this study can be found elsewhere.[23,24] With one of these systems (Clark-MXR, CPA 2210), it was possible to obtain a greater variability in terms of wavelength selection and to carry out intensity-dependent measurements. Briefly, one laser system

† Part of the special issue "Physical Chemistry of Ionic Liquids".

* To whom correspondence should be addressed. E-mail: andreas.unterreiner@ipc.uka.de.

10.1021/jp067163f CCC: $37.00
Published on Web 02/02/2007

SCHEME 1

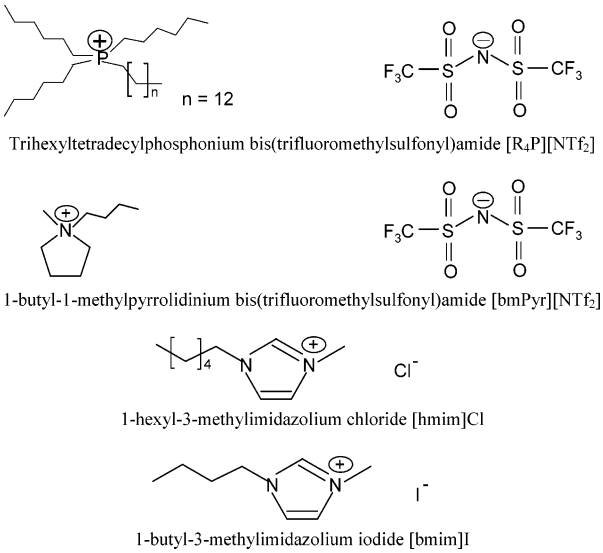

consisted of a home-built Ti:sapphire femtosecond laser oscillator and a regenerative amplifier (RGA) operating at 800 nm, while the second one was a fully integrated 1 kHz femtosecond laser system (Clark-MXR, CPA 2210) with a central wavelength of 775 nm. For generation of pump and probe pulses, the RGA outputs were split into two parts. UV pump pulses (λ = 258/266 nm, energy/pulse 0.1−16 μJ, time resolution $\approx$ 100 − 200 fs) were obtained by third harmonic generation of a portion of the RGA output. The other part of the RGA output was frequency doubled in a BBO to pump a home-built NOPA system according to the design published in reference 25 capable of delivering probe pulses from the visible to the NIR region. Two types of experiments were carried out with these systems: (i) step scan up to 100 ps averaging 200 data points of each delay stage and (ii) test of the photostability of RTILs by a rapid-scan method with only 20 data points per delay time. In order to study the pump intensity dependence, variable intensities between 1×10^8 and 25×10^8 W/cm^2 ($\lambda_{pump} \sim 258$ nm) were applied. In the pump−probe absorption studies, the change of the optical density with and without pump pulse (ΔOD) as a function of delay time was monitored. Positive ΔOD values correspond to pump-induced absorption. All measurements were carried out under nonfocused conditions of the pump pulse to avoid nonlinearities in the quartz cuvette. Reference measurements in these cuvettes without RTILs gave no transient response under these conditions. Continuous irradiation experiments were carried out by using a high-pressure Hg/Xe arc lamp (type LAX 1530, Müller).

All ILs were purchased from Merck/EMD in the highest available quality (pure/ultrapure). Ultrapure [R_4P][NTf_2] and [bmPyr][NTf_2] were further dried under vacuum at 80−90 °C to water contents below 1 ppm. The well-dried liquids were handled inside an argon-filled inert gas glovebox (H_2O, O_2 < 1 ppm) and subsequently sealed in quartz cuvettes with an optical path length of 1 mm. [hmim]Cl and [bmim]I were used as purchased (purity > 98%) and were filled in 1-mm cuvettes in an argon box. The viscosities of the ILs vary from ~80 mPa s[26] in the case of pyrrolidinium and phosphonium cation based ILs to about 400 mPa s for [bmim]I[27], whereas the viscosity of [hmim]Cl is about a factor of 45 higher than [bmim]I.[28]

3. Results

The structures of RTILs used in this investigation are given in Scheme 1. The stationary absorption spectra of [hmim]Cl and [bmim]I are shown Figure 1, while the spectra of phosphonium and pyrrolidinium cation based RTILs were published elsewehere.[4]

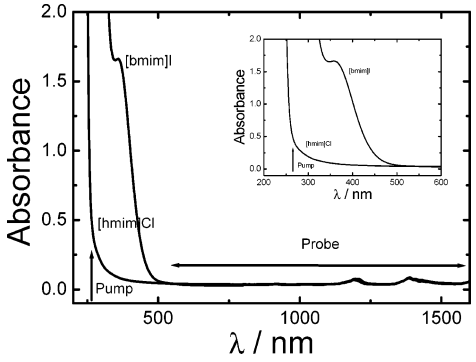

Figure 1. Static absorption spectra of the RTILs [hmim]Cl and [bmim]I. The pump wavelength (258 nm) and the probed wavelength region are indicated by arrows.

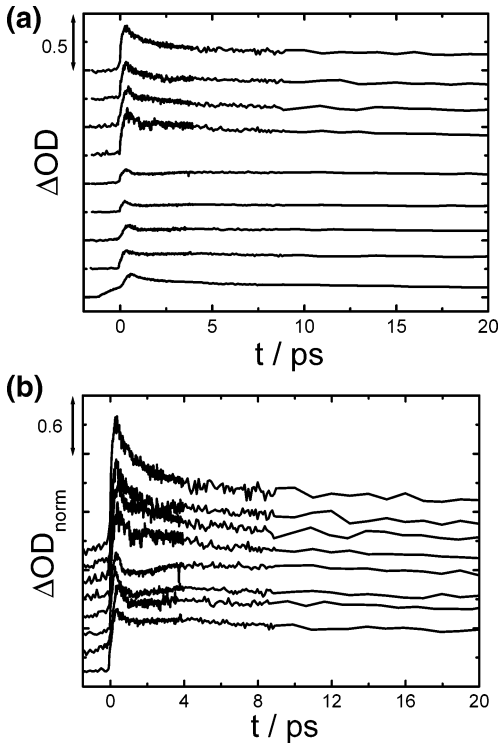

Figure 2. (a) Time-resolved induced absorption of solvated electrons generated by direct photolysis of [bmim]Cl. Probe wavelengths in nm from bottom to top: 700, 900, 1000, 1100 1200, 1300, 1400, 1500, and 1600. Transients are displaced in ΔOD for clarity. (b) Same as in (a) but the transients are normalized at long delay times (~100 ps). Probe wavelengths in nm from bottom to top: 900, 1000, 1100, 1200, 1300, 1400, 1500, and 1600. Pump energy $\approx 25 \times 10^8$ W/cm^2 at 258 nm.

3.1. Halide-Containing ILs. We first present results obtained from RTILs based on imidazolium cations. The transient response of pure [hmim]Cl after excitation with a 258-nm pulse (pulse duration $\approx$ 200 fs, energy $\approx$ 16 μJ per pulse) is shown in Figure 2a. The data represent induced absorption at various probe wavelengths collected with the step-scan method as described in the experimental section. The induced absorption data from Figure 2a are normalized at long delay times (~100 ps) and are displayed in Figure 2b. Similarly, the induced absorption at various probe wavelengths after excitation of [bmim]I by a 258-nm femtosecond UV pulse are shown in Figure 3a. We further show in Figure 3b normalized induced absorptions that are again displaced in ΔOD for clarity. To

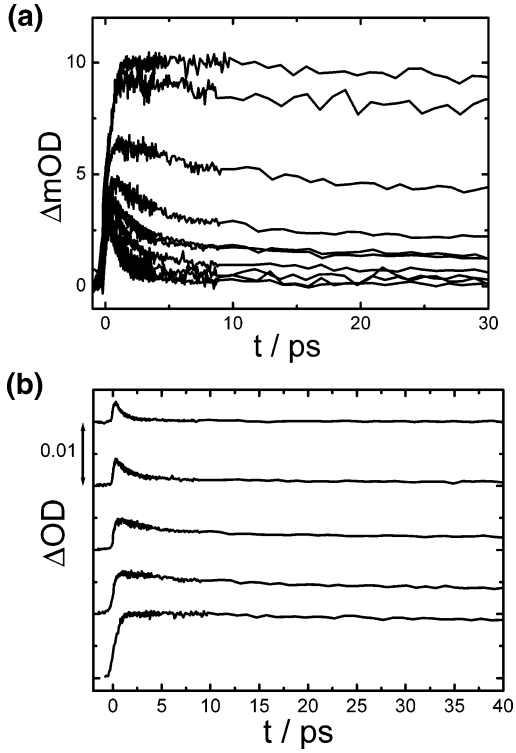

Figure 3. (a) Time-resolved induced absorption of solvated electrons generated by direct photolysis of [bmim]I. Probe wavelengths in nm from top to bottom: 555, 700, 900, 1000, 1100, 1200, 1300, 1400, 1500, and 1600. (b) For clarity some representative transients from (a) are displaced in ΔOD. Probe wavelengths in nm from bottom to top: 700, 900, 1000, 1300, and 1600.

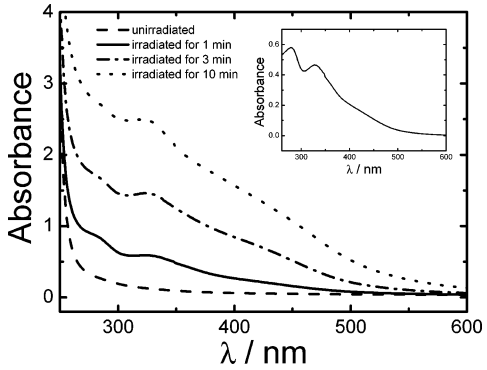

Figure 4. Absorption spectra of [bmim]Cl before and after irradiation with UV light at various times as shown in the figure. The inset shows the difference spectrum between a 1-min irradiated and unirradiated sample.

confirm the formation of di- and trihalide ions during irradiations by a femtosecond UV pulse (see discussion below), we irradiated a sample of [hmim]Cl in a 1-mm quartz cuvette with a high-pressure mercury/xenon arc lamp (type LAX 1530, Müller, maximum lamp power ≈ 300 W). After 1 min, the formation of Cl_3^- was indicated by a yellow color whose intensity increased with longer exposure to UV light (see Figure 4). For comparison the spectrum of the unirradiated sample is also shown. As can be seen the formation of Cl_3^- can be identified by two shoulders around 280 and 330 nm upon UV irradiation. Table 1 summarizes the observed absorption maxima of trihalides formed upon steady-state UV photolysis and femtosecond UV-irradiation experiments in the present study. Note that adding I_2 to [bmim]I (spectrum not shown) also gives an absorption peaking at 370 nm without irradiation of the sample. Addition of I_2 to iodide solutions is a well-known

TABLE 1: Absorption Band Maxima (λ) of Trihalides Formed in [hmim]Cl and [bmim]I upon Steady-State UV Photolysis and Femtosecond UV Laser Irradiation

	UV photolysis		femtosecond UV irradiation[a]	
IL	λ_1	λ_2	λ_1	λ_2
[hmim]Cl	280	330	280	325
[bmim]I	b	365	b	365

[a] Absorption spectrum of the sample was taken after femtosecond UV irradiation. [b] Peak was masked by solvent absorption.

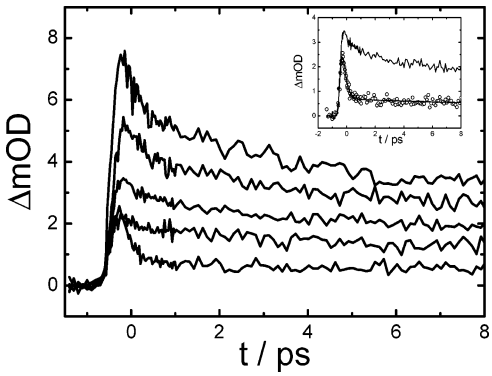

Figure 5. Time-dependent induced transient absorption at a probe wavelength of 900 nm after photolysis of [bmim]Cl collected with the help of rapid scans (see text for details). The illumination times in min from bottom to top are: 1, 3, 5, 25, and 80. The inset shows the first and third scans (1 and 5 min) clearly indicating the build-up of trichloride ions upon continuous irradiation.

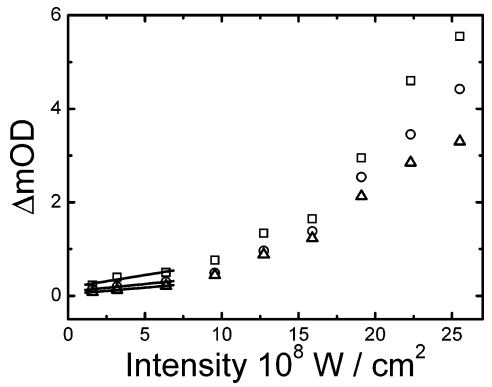

Figure 6. Maximum ΔOD values of the induced absorption after direct photolysis of [hmim]Cl as a function of pump intensity for various pump (258 nm) delay times at 900 nm. The solid line represents a linear fit.

process to generate I_3^-. To further support the formation of di- and trihalide ions upon continuous irradiation induced absorption data were collected with a rapid-scan method, and the results are shown in Figure 5. The increasing background on a picosecond time scale indicates the formation of these ions. Furthermore, intensity-dependent-induced absorption data were collected at a probe wavelength of 900 nm with laser intensities varying between 1×10^8 and 25×10^8 W/cm^2 (see Figure 6). To compare the recombination dynamics of solvated electrons in [hmim]Cl and [bmim]I, we show in Figure 7 induced absorptions at 1600 nm as probe wavelength.

3.2. ILs Containing Fluorinated Amide as Anion. The photoinduced reactions of halide-containing RTILs prompted us to further investigate pyrrolidinium and phosphonium amides. In an earlier work,[4,5] we have already demonstrated that fs UV-excitation led to the formation of solvated electrons. In the present study an extended probe wavelength region from 555 to 1500 nm was employed. The data for RTILs based on

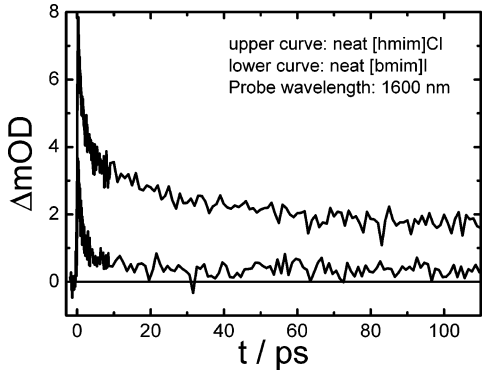

Figure 7. Induced absorption in [hmim]Cl and [bmim]I for comparison. Pump energy ≈ 16 μJ at 258 nm. Probe wavelength as shown in the figure.

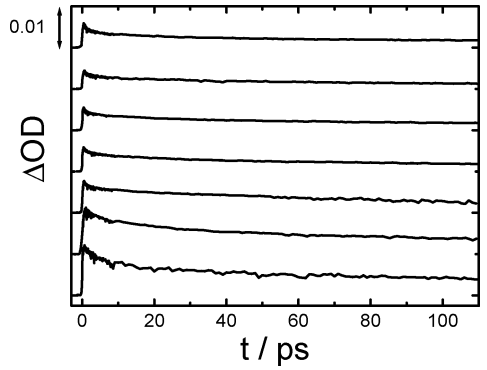

Figure 8. Time-dependent induced absorption of $[R_4P][NTf_2]$. Probe wavelengths from bottom to top: 555, 700, 900, 1000, 1100, 1300, and 1500 nm. Pump energy ≈ 16 μJ at 258 nm.

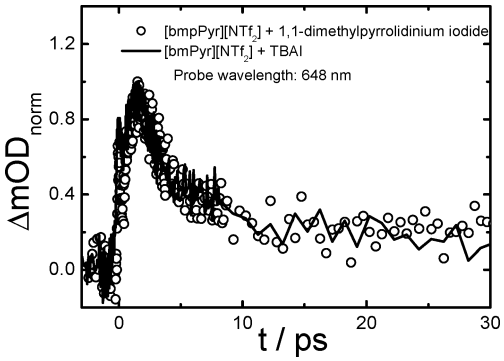

Figure 9. Time-dependent induced absorption of $[bmPyr][NTf_2]$ doped with TBAI and 1,1-dimethylpyrrolidinium iodide. Pump energy ≈ 1 μJ at 266 nm. Probe wavelength as shown in the figure.

phosphonium cation ($[R_4P][NTf_2]$) are displayed in Figure 8. The effect of doping the ILs with salts such as TBAI or dimethylpyrrolidnium iodide on the recombination dynamics was investigated in $[bmPyr][NTf_2]$ at other probe wavelengths as was done in our previous studies.[4] These results are shown in Figure 9. We also investigated the intensity dependence of the transient response of solvated electrons in $[R_4P][NTf_2]$, and the data are displayed in Figure 10 at 900 nm as probe wavelength.

4. Discussion

4.1. Ultrafast Photochemistry of Halide-Containing ILs. In this section, the generation and dynamics of solvated electrons as well as di- and trihalide ions are discussed after femtosecond UV photolysis of [hmim]Cl and [bmim]I.

4.1.1. Solvated Electrons vs Di- and Trihalide Ions. It is quite obvious from Figure 2a that the long-time behavior of

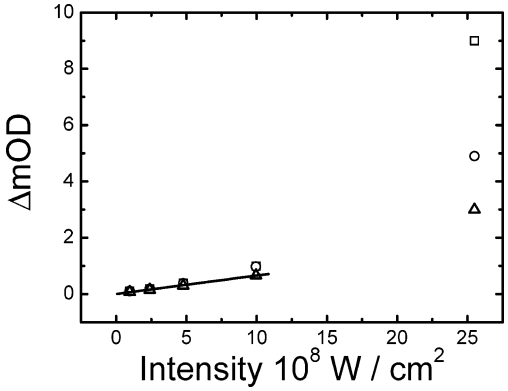

Figure 10. Maximum ΔOD values of the induced absorption after direct photolysis of $[R_4P][NTf_2]$ as a function of pump energy for various pump (258 nm) delay times at 900 nm. The solid line is a linear fit to the data.

the induced absorption is not identical at various wavelengths. Figure 2b further shows that the initial decay is followed by a small rise in the transient absorption at wavelengths between 700 and 1000 nm. Thereafter, the transients undergo a slow decay over hundreds of ps. Similar to the case of [hmim]Cl (parts a and b of Figure 2), we tentatively assign the immediate rise of the induced absorption in [bmim]I (Figure 3) to the formation of solvated electrons. With continuing irradiation—please note again that these experiments were carried out under static irradiation conditions, i.e., no sample replenishment between actinic events—di- and triiodide ion formation is also possible. Conclusively, di- and triiodide ions make noticeable contribution to the induced absorption only at shorter probe wavelengths (below 1000 nm) in both systems.

The immediate rise of ΔOD, especially at longer probe wavelengths (above 1000 nm), that can be exclusively attributed to solvated electrons (see below and section 4.1.2) indicates the existence of preformed cavities in RTILs in analogy to high-temperature ILs (HTILs) such as K−KCl.[29] This observation was also made in our previous studies with phosphonium and pyrrolidinium cation based RTILs.[4,5] It was shown previously by Parrinello and co-workers[30,31] that excess electrons localize in existing ionic cavities in HTILs. Wishart et al.[1] postulated a similar scenario for RTILs where electrons generated by pulse radiolysis localize in preformed aliphatic or hydroxylic domains depending on the type of ILs used. Furthermore, it was shown by MD simulations on structural and dynamical properties of imidazolium cation based ILs that cavity distributions exist in RTILs.[32] Also, the existence of such cavities and their detailed topography upon CO_2 dissolution was recently discussed by Huang et al.[33] However, the dependence of the electron localization on cavity distributions and sizes in RTILs is not well understood.

Our assignment of the induced absorption beyond 1000 nm to solvated electrons is further substantiated from studies by Neta and co-workers.[34] According to their results, solvated electrons generated by pulse radiolysis of deoxygenated solutions of [bmim]Cl with 2-propanol are rapidly scavenged by imidazolium cations with a rate constant of $\sim 1.9 \times 10^{10}$ L mol^{-1} s^{-1} giving rise to long-lived radicals peaking around 325 nm with a small shoulder near 350 nm. Earlier studies[35] on the reactions of hydrated electrons with imidazolium cations in aqueous solutions, however, reported rate constants that are 1 order of magnitude lower (3.9×10^9 L mol^{-1} s^{-1}) than those observed by Neta and co-workers. In the present study, such oxidized or reduced products should not make any significant contribution to the induced absorption observed between 555

and 1600 nm. However, di- and trihalide ions may partially contribute to the induced absorption at wavelengths between 555 and 1000 nm in both [hmim]Cl and [bmim]I in the present investigation as the absorption of these ions peaks at 330 and 750 nm. Beyond 1000 nm no contribution from these ions is expected as they do not have significant absorption bands above 1000 nm.[36,37] As a result, the transient response in [hmim]Cl and [bmim]I at shorter wavelengths can be ascribed to solvated electrons and di- and trichloride ions, the latter being formed upon continuous irradiation of ILs, while at wavelengths beyond 1000 nm the induced absorption may be safely attributed to solvated electrons alone.

Gamma ray radiolysis[38] of dialkylimidazolium chlorides also showed spectral changes with continuing irradiation affecting the entire spectrum below 540 nm. Among other possibilities the absorbance increase was attributed to the formation of the radical anion, $Cl_2^{\bullet -}$. The transient absorption which peaks near 325 nm in pure imidazolium ILs was attributed to a large number of radiolytic products, which all have more or less the same absorption spectrum.[34] From these findings together with our present observations we postulate the following reaction mechanism. Solvated electrons are generated from halide ions of the RTILs according to

$$X^- \xrightarrow{h\nu} X + e_{solv}^- \ (X = Cl \text{ or } I) \qquad (1)$$

Immediately after excitation, (geminate) recombination occurs via

$$X + e_{solv}^- \rightarrow X^- \qquad (2)$$

Thereafter—on a much longer time scale (at least several tens of nanoseconds)—the formation of dihalide ions proceeds via

$$X + X^- \rightarrow X_2^- \qquad (3)$$

It is known that the lifetime of dihalide ions exceeds that of solvated electrons in salt doped polar liquids.[39] For example, the lifetime of solvated electrons was found to be about 110 ns in a solution of glycerol with potassium iodide, while that of diiodide extended up to 500 μs.[40] In the present study, we observe the formation of trihalide ions ($2X_2^- \rightarrow X_3^- + X^-$) indicated by a yellow color after continuous femtosecond UV laser irradiation. As explained above, this formation is characterized by two absorption bands peaking around 280 and 330 nm (see Table 1). Note that the spectra of the irradiated samples were taken after femtosecond UV irradiation. Figure 4 displays the spectra of the steady-state UV-irradiated samples of [hmim]-Cl. For comparison the spectrum of the unirradiated sample is also shown. As can be seen the formation of Cl_3^- can be identified by two shoulders around 280 and 330 nm upon UV irradiation also indicated by a yellow color that has already appeared after 1 min of irradiation. The two absorption bands are more pronounced in the difference spectra of irradiated and unirradiated samples (see inset of Figure 4). On the other hand, the dihalide ion (e.g., I_2^-) has two absorption maxima, one at 320 nm and the other around 740 nm. Note that, due to the short lifetime, these two bands cannot be seen under steady-state photolysis.

Two strategies may help avoiding the trihalide ion formation in ILs: (i) a flow cell system and (ii) rapid-scan method according to the design by Feldstein et al.[41] The first method is currently not viable due to the high viscosity of RTILs. The second method had to be refined because of the low amplitudes of the induced absorption in RTILs. Therefore, 20 data points were collected at each delay step of 20 fs. This procedure reduced the overall exposure time of the samples from 20 min required in the step-scan method to 1 min. Figure 5 shows exemplarily transients at a probe wavelength of 900 nm recorded with the rapid-scan method. As can be seen, there is a pulse-limited rise of the induced absorption, which is followed by a biexponential decay. This trend continues and the transients reach their maximum amplitude after about 50 min of irradiation. There are, however, clear differences in the nature of the transients as can be seen in the inset of Figure 5. For example, a major fraction of the induced absorption recorded in the very first scan undergoes a fast decay suggesting that mostly solvated electrons are generated which are subject to an efficient recombination. In contrast, the transients recorded during the subsequent scans undergo only a partial decay. Although reaction 3 is very slow compared to reaction 2 (recombination reaction) progressive rapid scans led to an increase of the di- and trihalide concentrations via reaction 3. This experiment clearly demonstrates that under continuous irradiation conditions solvated electrons as well as di- and trihalide ions are generated in [hmim]Cl and [bmim]I ILs. However, the contribution of these halides to the dynamics of RTILs after photoexcitation is only significant at shorter probe wavelengths. On the other hand, when the samples are irradiated only for a short time (e.g., first scan in Figure 5) di- and trihalide formation is negligible. Further evidence for the formation of these ions is given by laser intensity-dependent measurements of the induced absorption (see next paragraph).

Therefore, transients at a probe wavelength of 900 nm were recorded with pump intensities between 1×10^8 and 25×10^8 W/cm^2. Figure 6 shows the maximum ΔOD of the transients as a function of pump intensity for various pump−probe delays. Within the experimental errors, the induced absorption increases linearly up to about 6×10^8 W/cm^2 suggesting a one-photon process for the formation of solvated electrons according to reaction 1. However, as the laser intensity is increased beyond this value the induced absorption does not follow the linear relationship with intensity any longer. Instead a nonlinear behavior, i.e., a change of the slope with varying delay times, is observed at all pump−probe delays. From this finding we conclude that with increasing laser intensity the concentration of solvated electrons increases along with that of halide radicals according to reaction 1, whereas at higher intensities the photochemistry of trihalides has to be considered, too. Finally, a comparison of the data of the two imidazolium halides suggests that [hmim]Cl is photolytically more unstable than [bmim]I and that both RTILs undergo degradation during photolysis leading to the formation of long-lived intermediates.

4.1.2. Dynamics of Solvated Electrons in [hmim]Cl and [bmim]I. Our assignment of the induced absorption to the solvated electrons at longer probe wavelengths may be further supported by studies from the literature. Similar observations of wavelength-dependent-induced absorption dynamics of solvated electrons were made in the case of nonpolar liquids.[42] For example, in alkanes, the initial rise of the induced absorption at 800, 1500, and 2250 nm after UV excitation was attributed to the formation of solvated electrons along with other intermediates. In the presence of 2.2 M of CCl_4, a good electron scavenger, the transient at 800 nm was found to undergo only a partial decay, which was in contrast to that observed at probe wavelengths of 1500 nm or 2250 nm where the transient decayed completely with a time constant of <1 ps.[42] The residual transient absorption at 800 nm in the presence of CCl_4 was explained on the basis of the contribution to the transient of

intermediates such as, for example, *n*-hexane cations, which have a broad absorption band with a maximum around 520 nm and extending beyond 1200 nm. On the basis of these observations, the induced absorption at 1500 and 2250 nm was attributed exclusively to solvated electrons. From these studies and those from Wishart and Neta[5] where the absorption band of solvated electrons was reported to extend beyond 1600 nm, we conclude that in the present investigation solvated electrons contribute to the induced absorption observed at wavelengths between 555 and 1600 nm in [hmim]Cl and [bmimi]I either partially (below 1000 nm) or completely (beyond 1000 nm).

It is obvious from the discussion above that di- and trihalide ions make a significant contribution to the observed induced absorption only at shorter probe wavelengths, while that of solvated electrons increases as the wavelengths are tuned farther into NIR region. As a result, the induced absorption measured above 1000 nm can be attributed to solvated electrons exclusively. However, the ultrafast dynamics of solvated electrons appear to depend strongly on the type of halide as a counterion in ILs. Figure 7 shows induced absorptions at 1600 nm as probe wavelength in [hmim]Cl and [bmim]I. It can be clearly seen that the fraction of solvated electrons undergoing decay is different in both imidazolium ILs. Solvated electrons undergo very efficient geminate recombination in the case of [bmim]I where the decay is almost complete within about 1 ps, whereas it is slower in the case of [hmim]Cl (only about 50% decay after ~2 ps). Kloepfer et al.[43] reported that much larger fractions of solvated electrons generated by a one-photon detachment of iodide in various "normal" solvents undergo geminate recombination compared to the chloride system. They attributed this to a faster nonadiabatic reverse electron-transfer reaction for iodide. We[4] have already reported such an efficient geminate recombination of solvated electrons when RTILs were doped with either pyrrolidinium iodide or TBAI.

The recombination dynamics in the present study with imidazolium ILs (Figure 7) can be further explained on the basis of the length of alkyl chain on the cation by comparison with ultrafast dynamics of alkanes. The geminate recombination reactions between solvated electrons and the solvent cation were found to be faster in *n*-hexane compared to *n*-octane.[39] The dynamics of solvated electrons in these liquids are controlled by the mutual diffusion of the parent cation and the electron. As a result, geminate recombination of solvated electrons further depends on their mobility in a solvent. The faster recombination dynamics in *n*-hexane compared to *n*-octane were attributed to a higher electron mobility in the former. For instance, the electron mobility in *n*-hexane is reported to be higher than in *n*-octane by more than a factor of 2.[44] Accordingly, the efficient recombination dynamics in [bmim]I may be due to a higher electron mobility compared to [hmim]Cl. Viscosity is another property that influences the electron mobilities and hence the recombination dynamics of solvated electrons in ILs. The viscosity of ILs depends on the alkyl chain length (the longer the chain length the higher the viscosity).[45] The very high viscosity of [hmim]Cl (a factor of 45 higher than [bmim]I) will no doubt reduce the electron mobility making the recombination reaction inefficient. To further enlighten this issue, future studies on ultrafast dynamics in RTILs should concentrate on recombination dynamics of solvated electrons in a series of RTILs with chain-length varying alkyl groups as substituents and temperature-dependent studies in jet-flow systems of ILs.

4.2. Ultrafast Photochemistry of ILs Containing Fluorinated Amide as Anion. The nature of the transient response in $[R_4P][NTf_2]$ at all probe wavelengths is identical to those reported by us previously.[4] Only a small fraction of induced absorption undergoes a fast decay, while the residual response remains more or less unchanged for hundreds of ps. This further proves a long lifetime of solvated electrons and is in good agreement with results by Wishart and Neta.[2] In the presence of additives such as TBAI and 1,1-dimethylpyrrolidinium iodide, a major fraction (>70%) of the transient in $[bmPyr][NTf_2]$ decays within about 3 ps, suggesting an efficient recombination of solvated electrons with iodine atoms. In comparison with the results for [bmim]I, this is a further confirmation of a faster and efficient recombination of solvated electrons with iodine atoms. Furthermore, geminate recombination depends neither on the purity of ILs nor on the doped salt as long as the dopant is an iodide derivative. This is demonstrated in Figure 9 at a probe wavelength of 648 nm for $[bmPyr][NTf_2]$ doped with TBAI and 1,1-dimethylpyrrolidinium iodide. Here, two samples of $[bmPyr][NTf_2]$ with varying purity have been employed: One is a high-purity sample that was further purified (see Experimental section for details on purification) and the other one (~98% purity) was used directly without any further purification. As can be seen, neither the nature nor the dynamics depend on the quality of the ILs employed. Furthermore, the induced absorption in Figure 9 is identical to another probe wavelength that has previously been published.[4] These findings suggest that the dynamics within 10 ps are dominated by reaction 2 ($I + e^- \rightarrow I^-$) and impurities do not play any role.

As in the case of imidazolium ILs, $[bmPyr][NTf_2]$ and $[R_4P][NTf_2]$ are found to slowly turn yellow with increasing irradiation times suggesting degradation of these liquids to unknown products during photolysis. To verify the degradation we recorded intensity-dependent transients (Figure 10). The results are similar to those found for both [hmim]Cl and [bmim]I. Up to about 10×10^8 W/cm^2 pump intensity the linear increase of the induced absorption suggests a one-photon process for the generation of solvated electrons. However, the induced absorption becomes nonlinear thereafter which may be due to an extra contribution of the induced absorption from long-lived degradation products of the ILs. In contrast to halide-containing RTILs, no absorption around 740 nm was found but only a red shift of the UV band being responsible for the yellow color. Here, further experiments, especially a photoproduct analysis, are necessary.

5. Conclusions

In this study, the ultrafast dynamics of various pure and salt-doped RTILs upon UV excitation were explored using a femtosecond pump−probe optical absorption technique as well as continuous UV light irradiation. The formation of solvated electrons was indicated by a pulse duration limited rise of the induced absorption at all probe wavelengths. This rise was followed by a decay attributable to geminate recombination of solvated electrons. In the presence of additives such as TBAI and 1,1-dimethylpyrrolidinium iodide geminate recombination dominates leading to a short lifetime of solvated electrons of about 2 ps. UV photolysis of imidazolium ILs led to the formation of di- and trihalides disturbing the dynamics of solvated electrons below 1000 nm. The rapid-scan technique demonstrated that RTILs are subject to photoinduced build-up of various compounds under static irradiation conditions. In the case of pyrrolidinium- and phosphonium-based RTILs the photoinduced degradation suggests alternative mechanisms. As a result, future ultrafast investigations should envisage the use of flow-cell systems to exchange the RTILs after subsequent

laser shots. However, the high viscosity of some of these liquids represents a severe limitation of the applicability. Concerning the technical applications of RTILs proper photoinduced studies are urgently needed to explore the photochemical processes in more detail.

Acknowledgment. We thank the Deutsche Forschungsgemeinschaft (Project UN 108) for financial support of this work. We gratefully acknowledge the help of Prof. F. Endres from the University of Clausthal-Zellerfeld providing us with a carefully purified sample of the IL [bmPyr][NTf_2] doped with 1,1-dimethylpyrrolidinium iodide. A.N.U. thanks the Dr. Otto-Röhm-Gedächtnisstiftung for partly funding this research and Prof. Dr. H. Hippler for his generous support of this work.

References and Notes

(1) Wishart, J. F.; Lall-Ramnarian, S. I.; Raju, R.; Scumpia, A.; Bellevue, S.; Ragbir, R.; Engel, R. *Radiat. Phys. Chem.* **2005**, *72*, 99 and references cited therein.
(2) Wishart, J. F.; Neta, P. *J. Phys. Chem. B* **2003**, *107*, 7261.
(3) Behar, D.; Neta, P.; Schultheisz, C. *J. Phys. Chem. A* **2002**, *106*, 3139.
(4) Chandrasekhar, N.; Endres, F.; Unterreiner, A. N. *Phys. Chem. Chem. Phys.* **2006**, *8*, 3192.
(5) Chandrasekhar, N.; Unterreiner, A. *N. Z. Phys. Chem.* **2006**, *220*, 1235.
(6) Welton, T. *Chem. Rev.* **1999**, *99*, 2071.
(7) Wilkes, J. S.; Zawarotko, M. J. *J. Chem. Soc. Chem. Comm.* **1992**, 965.
(8) Kuang, D.; Ito, S.; Wenger, B.; Klein, C.; Moser, J. E.; Baker, R. H.; Zakeerudiin, S. M.; Grätzel, M. *J. Am. Chem. Soc.* **2006**, *128*, 4146 and references cited therein.
(9) Mazille, F.; Fei, Z.; Kuang, D.; Zhao, D.; Nazeeruddin, S. M.; Grätzel, M.; Dyson, J. P. *Inorg. Chem.* **2006**, *45*, 1585.
(10) Kawano, R.; Watanabe, M. *Chem. Comm.* **2005**, 2107.
(11) Sakaebe, H.; Matsumoto, H. *Electrochem. Commun.* **2003**, *5*, 594 and references cited therein.
(12) Nada, A.; Susan, M. A. B. H.; Kudo, K.; Mitsushima, S.; Hayamizu, K.; Watanabe, M. *J. Phys. Chem. B* **2003**, *107*, 4024.
(13) Nanjundiah, C.; McDevitt, S. F.; Koch, V. R. *J. Electrochem. Soc.* **1997**, *144*, 3392.
(14) Kubo, W.; Kambe, S.; Nakade, S.; Kitamura, T.; Hanabusa, K.; Wada, Y.; Yanagida, S. *J. Phys. Chem. B* **2003**, *107*, 4374.
(15) Wang, P.; Zakeeruddin, S. M.; Moser, J. E.; Grätzel, M. *J. Phys. Chem. B.* **2003**, *107*, 13280.
(16) O'Regan, B.; Grätzel, M. *Nature* **1991**, *353*, 737.
(17) Hagfeldt, A.; Grätzel, M. *Chem. Rev.* 1995, 95, 49.
(18) Hagfeldt, A.; Grätzel, M. *Acc. Chem. Res.* 2000, 33, 269.
(19) Grätzel, M. *Nature* 2001, 414, 338.
(20) Hara, K.; Nishikawa, T.; Kurashige, M.; Kawauchi, H.; Kashima, T.; Sayama, K.; Aika, K.; Arakawa, H. *J. Phys. Chem. B* **2002**, *106*, 12693.
(21) Wang, P.; Zakeeruddin, S. M.; Baker, R. H.; Grätzel, M. *Chem. Mater.* **2004**, *16*, 2694.
(22) Ozawa, R.; Hamagushi, H. *Advances in Chemical Physics*; John Wiley & Sons; New York, 2005; Vol. 131.
(23) Unterreiner, A. N. Ph.D. Thesis, Universität Karlsruhe, 1998, ISBN 3-89653-368-1.
(24) Ehrler, O. T.; Yang, J. P.; Hättig, C.; Unterreiner, A. N.; Hippler, H.; Kappes, M. M. *J. Chem. Phys.* **2006**, *125*, 074312.
(25) Piel, J.; Beutter, M.; Riedle, E. *Opt. Lett.* **2000**, *25*, 180.
(26) Zhou, Z. B.; Matsumoto, H.; Tatsumi, K. *Chem.−Eur. J.* **2006**, *12*, 2196.
(27) Kim, K. S.; Demberelnyamba, D.; Shin, B. K.; Yeon, S. H.; Choi, S.; Cha, J. H.; Lee, H.; Lee, C. S.; Shim, J. J. *Kor. J. Chem. Eng.* **2006**, *23*, 113.
(28) Gomez, E.; Gonzalez, B.; Domniquez, A.; Tojo, E.; Tojo, J. *J. Chem. Eng. Data* **2006**, *51*, 696.
(29) Freyland, W.; Garbade, H.; Pfeiffer, E. *J. Phys. Chem.* **1984**, *88*, 3745.
(30) Selloni, A.; Carnevali, P.; Car, R.; Parrinello, M. *Phys. Rev. Lett.* **1987**, *59*, 823.
(31) Fois, E. S.; Selloni, A.; Parrinello, M.; Car, R. *J. Phys. Chem.* **1988**, *92*, 3268.
(32) Margulis, C. J. *Mol. Phys.* **2004**, *102*, 829.
(33) Huang, X.; Margulis, C. J.; Li, Y.; Berne, B. J. *J. Am. Chem. Soc.* **2005**, *127*, 17842.
(34) Behar, D.; Gonzales, C.; Neta, P. J. *Phys. Chem. A* **2001**, *105*, 7607.
(35) Buxton, G. V.; Greenstock, G. L.; Helman, W. P.; Ross, A. B. *J. Phys. Chem. Ref. Data* **1988**, *17*, 513.
(36) Gershgoren, E.; Gordon, E.; Ruhman, S. *J. Chem. Phys.* **1997**, *106*, 4806.
(37) Gershgoren, E.; Banin, U.; Ruhman, S. *J. Phys. Chem. A* **1998**, *102*, 9.
(38) Allen, D.; Baston, G.; Bradley, A. E.; Gorman, T.; Haile, A.; Hamblett, I.; Hatter, J. E.; Healey, M. J. F.; Hodgson, B.; Lewin, R.; Lovell, K. V.; Newton, B.; Pitner, W. R.; Rooney, D. W.; Sanders, D.; Seddon, K. R.; Sims, H. E.; Thied, R. C. *Phys. Chem. Chem. Phys.* **2002**, *4*, 152.
(39) Assad, A. N.; Chandrasekhar, N.; Nashed, A. W.; Krebs, P. *J. Phys. Chem. A* **1999**, *103*, 6339.
(40) Chandrasekhar, N.; Krebs, P. *J. Chem. Phys.* **2000**, *112*, 5910.
(41) Feldstein, M. J.; Voehringer, P.; Scherer, N. F. *J. Opt. Soc. Am. B* **1995**, *12*, 1500.
(42) Siebbeles, L. D. A.; Emmerichs, U.; Hummel, A.; Bakker, H. J. *J. Chem. Phys.* **1997**, *107*, 9339.
(43) Kloepfer, J. A.; Vichiz, V. H.; Lenchenkov, V. A.; Germaine, A. C.; Bradforth, S. E. *J. Chem. Phys.* **2000**, *113*, 6288.
(44) Long, F. H.; Lu, H.; Eisenthal, K. B. *J. Phys. Chem.* **1995**, *99*, 7436.
(45) Tokuda, H.; Hayamizu, K.; Ishii, K.; Susan, M. A. B. H.; Watanabe, M. *J. Phys. Chem. B* **2005**, *109*, 6103.